

## MIT Open Access Articles

*The Extreme Anterior Domain Is an Essential Craniofacial Organizer Acting through Kinin-Kallikrein Signaling*

The MIT Faculty has made this article openly available. **Please share** how this access benefits you. Your story matters.

**Citation:** Jacox, Laura, Radek Sindelka, Justin Chen, Alyssa Rothman, Amanda Dickinson, and Hazel Sive. "The Extreme Anterior Domain Is an Essential Craniofacial Organizer Acting through Kinin-Kallikrein Signaling." *Cell Reports* 8, no. 2 (July 2014): 596–609.

**As Published:** <http://dx.doi.org/10.1016/j.celrep.2014.06.026>

**Publisher:** Elsevier

**Persistent URL:** <http://hdl.handle.net/1721.1/96821>

**Version:** Final published version: final published article, as it appeared in a journal, conference proceedings, or other formally published context

**Terms of use:** Creative Commons Attribution-NonCommercial-NoDerivs 3.0 Unported License



# The Extreme Anterior Domain Is an Essential Craniofacial Organizer Acting through Kinin-Kallikrein Signaling

Laura Jacox,<sup>1,2,3,4,5,6</sup> Radek Sindelka,<sup>1,6,7</sup> Justin Chen,<sup>1,2</sup> Alyssa Rothman,<sup>1</sup> Amanda Dickinson,<sup>1,8</sup> and Hazel Sive<sup>1,2,\*</sup>

<sup>1</sup>Whitehead Institute for Biomedical Research, Nine Cambridge Center, Cambridge, MA 02142, USA

<sup>2</sup>Massachusetts Institute of Technology, 77 Massachusetts Ave, Cambridge, MA 02139, USA

<sup>3</sup>Harvard School of Dental Medicine, 188 Longwood Avenue, Boston, MA 02115, USA

<sup>4</sup>Harvard Medical School, 250 Longwood Avenue, Boston, MA 02115, USA

<sup>5</sup>Harvard Graduate School of Arts and Sciences, 1350 Massachusetts Avenue, Holyoke Center, 50, Cambridge, MA 02138, USA

<sup>6</sup>Co-first author

<sup>7</sup>Present address: Institute of Biotechnology, Videnska 1083, Prague 4, 14220, Czech Republic

<sup>8</sup>Present address: Virginia Commonwealth University, 1000 West Cary Street, Richmond, VA 23284, USA

\*Correspondence: [sive@wi.mit.edu](mailto:sive@wi.mit.edu)

<http://dx.doi.org/10.1016/j.celrep.2014.06.026>

This is an open access article under the CC BY-NC-ND license (<http://creativecommons.org/licenses/by-nc-nd/3.0/>).

## SUMMARY

The extreme anterior domain (EAD) is a conserved embryonic region that includes the presumptive mouth. We show that the Kinin-Kallikrein pathway is active in the EAD and necessary for craniofacial development in *Xenopus* and zebrafish. The mouth failed to form and neural crest (NC) development and migration was abnormal after loss of function (LOF) in the pathway genes *kng*, encoding Bradykinin (xBdk), *carboxypeptidase-N* (*cpn*), which cleaves Bradykinin, and *neuronal nitric oxide synthase* (*nNOS*). Consistent with a role for nitric oxide (NO) in face formation, endogenous NO levels declined after LOF in pathway genes, but these were restored and a normal face formed after medial implantation of xBdk-beads into LOF embryos. Facial transplants demonstrated that Cpn function from within the EAD is necessary for the migration of first arch cranial NC into the face and for promoting mouth opening. The study identifies the EAD as an essential craniofacial organizer acting through Kinin-Kallikrein signaling.

## INTRODUCTION

The face derives from both neural crest and nonneural crest derivatives. The presumptive mouth arises from a conserved extreme anterior domain (EAD) where ectoderm and endoderm are juxtaposed (Dickinson and Sive, 2006). The cranial neural crest (NC) migrates into the future facial region to abut the EAD (Dickinson and Sive, 2007; Spokony et al., 2002) during tail bud stages in *Xenopus*. At mouth opening, the cranial NC has begun differentiating into cranial nerves, melanocytes, connective tissue, and chondrocytes that contribute to the jaws and other facial bones (Santagati and Rijli, 2003). The EAD expresses signaling regulators (Dickinson and Sive, 2009), which sug-

gested that the region might act as a facial organizer. We addressed this possibility using transplant assays where EAD lacking the secreted Wnt regulators Frzb1 and Crescent replaced the EAD of a control embryo. Not only did the mouth fail to form, but surrounding facial regions appeared abnormal, suggesting more global activity of the EAD. However, this putative organizer activity was not extensively explored for other factors impacting mouth formation and cranial NC migration.

Molecular rules for NC movement have been extensively described and include contact inhibition of locomotion, coattraction, chase-and-run strategies (Theveneau et al., 2013), and guidance through interaction with extracellular matrix, semaphorins, and Eph/Ephrin signals (Mayor and Theveneau, 2013). Despite these elegant conclusions, the mechanisms that direct the cranial NC into the face primordium, and the identity of localized guidance signals that facilitate this migration are not known.

In a microarray screen to identify regulatory genes expressed in the EAD that may regulate mouth and other aspects of face formation, we isolated *carboxypeptidase N* (*cpn*), *kininogen* (*kng*), and *neuronal nitric oxide synthase* (*nNOS*). These genes are members of the Kinin-Kallikrein pathway (Kakoki and Smithies, 2009), a regulator of blood pressure (Sharma, 2009) that also participates in inflammation (Bryant and Shariat-Madar, 2009) and renal function. This pathway had not been described as necessary for craniofacial development in any animal. In the adult mammalian Kinin-Kallikrein pathway (Figure 1A), Kallikrein, a protease, cleaves KNG to yield Bradykinin, a 9 amino acid (9AA) peptide. Bradykinin is a vasodilator that binds the Bradykinin B2 (BKB2) G-protein-coupled receptor. BKB2 receptor activates NOS, which converts L-Arginine (Arg) to nitric oxide (NO) and citrulline. Bradykinin can also be cleaved by CPN, yielding 8AA desArg-Bradykinin and Arg that can be converted to NO (Moncada and Higgs, 1995). The BKB2 receptor is constitutively expressed in adult mammals and binds Bradykinin, but not desArg-Bradykinin, to activate NOS (Kakoki and Smithies, 2009). A BKB1 receptor is conditionally expressed during inflammation and binds desArg-Bradykinin but not Bradykinin. Angiotensin Converting Enzyme (ACE) degrades both Bradykinin and desArg-Bradykinin.

### A Mammalian Kinin-Kallikrein Pathway

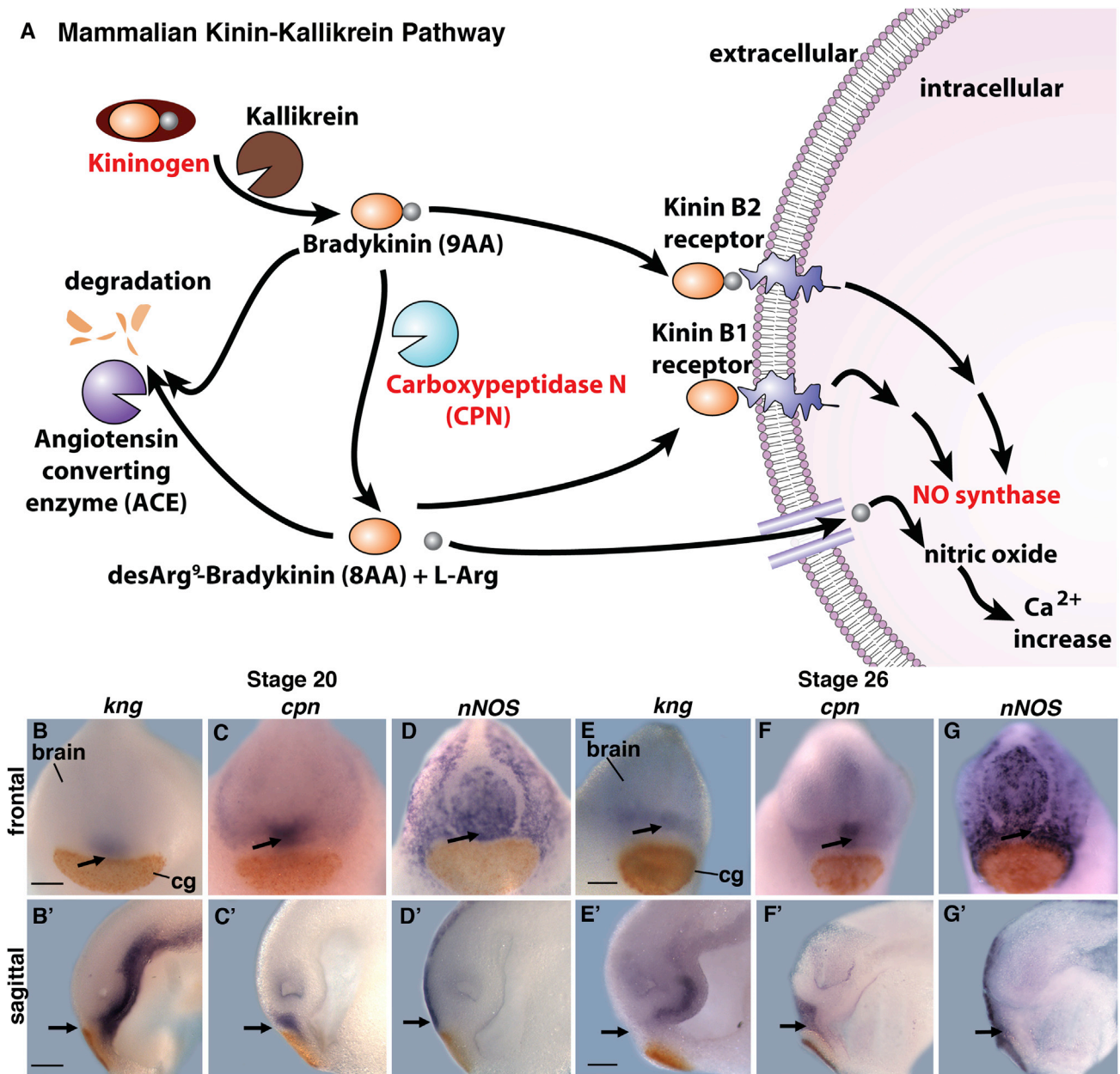


**Figure 1. Mammalian Kinin-Kallikrein Pathway and Putative Pathway Genes Are Expressed in the Developing Face**

(A) Adult mammalian Kinin-Kallikrein pathway (Kakoki and Smithies 2009).

(B–G) In situ hybridization for *kng* (B, B', E, and E'), *cpn* (C, C', F, and F'), and *nNOS* RNA (D, D', G, and G') (RNA is purple). Cement gland marker (*xcg*) is red. Arrow: presumptive mouth. cg, cement gland. (B–G) frontal views; (B'–G') sagittal sections. Scale bars, 200 μm.

In addition to its role in the Kinin-Kallikrein pathway, NO participates in multiple processes including wound healing, tissue regeneration (Filippin et al., 2011), angiogenesis (Cooke, 2003), neurotransmission (Contestabile and Ciani, 2004), and possibly malignancy (Olson and Garban, 2008). NO has been implicated in developmental contexts including neuronal development (Bradley et al., 2010), bone growth regulation, (Yan et al., 2010), cardiac endothelial-to-mesenchymal transition (Chang et al., 2011), and control of organ size and developmental timing

(Kuzin et al., 1996). Elevated NO production has been found in developing epithelial tissues, ganglia, and the notochord (Lepiller et al., 2007). In *Xenopus*, NO is a potent parthenogenetic activator of *Xenopus* eggs (Jeseta et al., 2012) and is correlated with movement in tadpoles (McLean and Sillar, 2000).

The strong expression of *kng*, *cpn*, and *nNOS* in the EAD led us to hypothesize that the Kinin-Kallikrein pathway is active during embryogenesis and required for facial development. We present data that support this hypothesis, and additionally show that

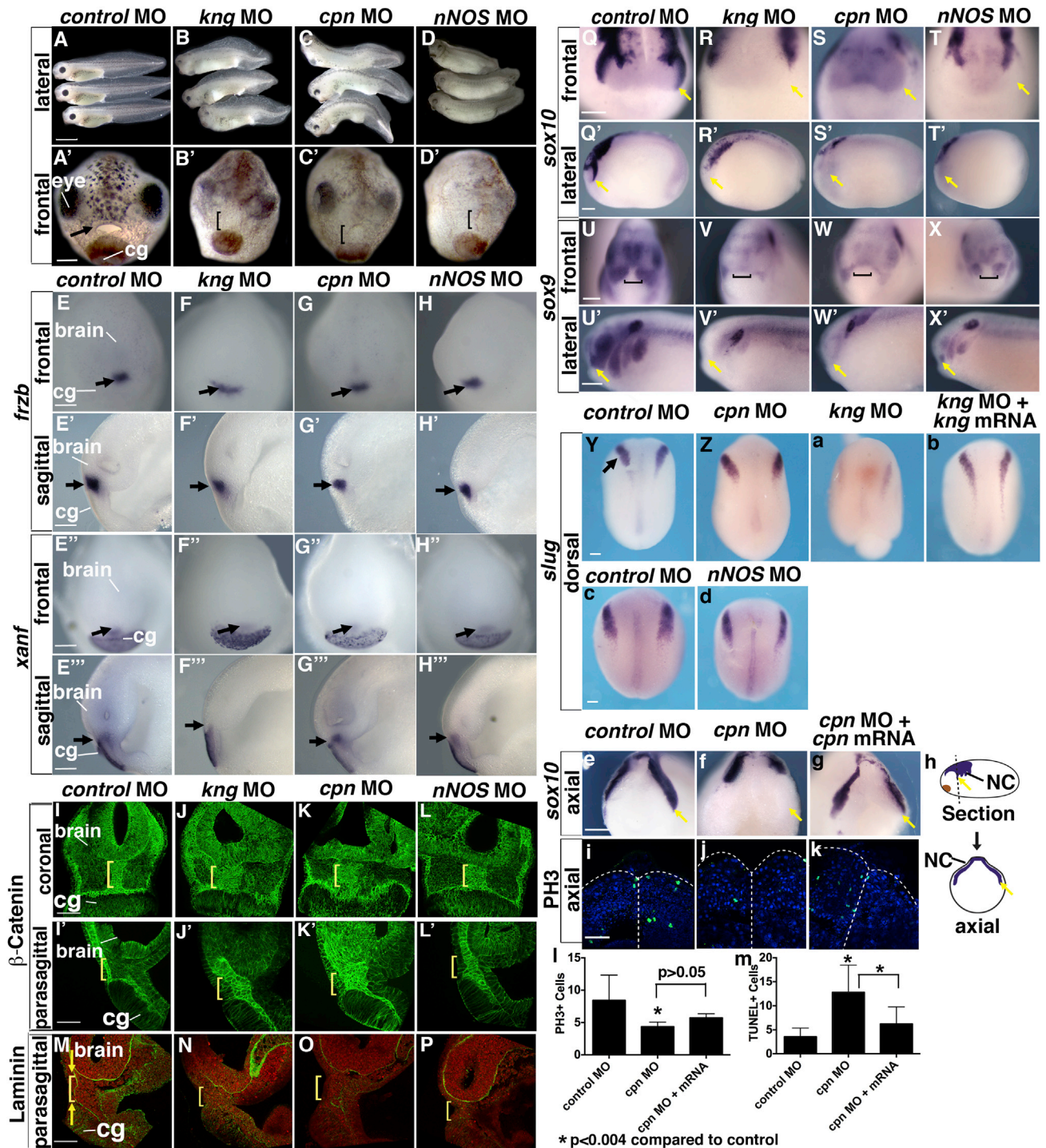


**Figure 2. *kng*, *cpn*, and *nNOS* Are Required for Mouth Opening and Face Formation**

(A–D') *kng*, *cpn*, and *nNOS* loss of function (LOF) using antisense morpholinos. Embryos assayed at stage 40, in four independent experiments. Arrow: mouth region. Bracket: unopened mouth. cg, cement gland. Scale bar in (A–D), 2,000  $\mu$ m. Scale bar in (A'–D'), 200  $\mu$ m. (A and A') Control morphants (100% normal, n = 97). (B–D') *kng*, *cpn*, and *nNOS* morphants (*kng* [B'] 0% normal, n = 102; *cpn* [C'] 2% normal, n = 105; *nNOS* [D'] 0% normal, n = 129). (E–H'') Kinin-Kallikrein pathway morphants at stage 22 express presumptive mouth markers, *frzb1* and *xanf1*. Scale bars, 200  $\mu$ m. (I–P and I'–L') Histology of *kng*, *cpn*, and *nNOS* LOF. Coronal sections (I–L, control morphant 100% normal, n = 5; each Kinin-Kallikrein morphant, 0% normal, n = 9) assayed at stage 26 in two independent experiments with  $\beta$ -catenin immunolabeling. Parasagittal sections with anterior to the left (I'–L', control morpholino 100% normal, n = 5; each Kinin-Kallikrein pathway morpholino, 0% normal, n = 12).

(legend continued on next page)

Kinin-Kallikrein signaling localized to the EAD is necessary for movement of the first arch cranial NC into the face, and for mouth formation. The study identifies the EAD as an essential craniofacial organizing center acting through Kinin-Kallikrein signaling.

## RESULTS

### ***kininogen, carboxypeptidase N, and neural nitric oxide synthase Are Expressed in the EAD during Initial Stages of Craniofacial Development***

*kng*, *cpn*, and *nNOS* expression was identified in the *Xenopus* EAD region (Dickinson and Sive, 2009; Figure S1A), suggesting activity of an embryonic Kinin-Kallikrein pathway (Figure 1A). Protein alignment showed high conservation of Cpn and nNOS (Figures S1B–S1D). Gene expression was examined by in situ hybridization and quantitative RT-PCR (qPCR) (Figures 1B–1G' and S1E–S1G). At tail bud (stages 20 and 26) when the EAD is present and cranial NC is migrating, *kng* is expressed in the prechordal plate with anterior expression adjacent to the EAD (Figures 1B, 1B', 1E, and 1E'). At stage 20, *cpn* was expressed in deep EAD layers (Figures 1C and 1C') and by stage 26 at low intensity in the first branchial arch (Figures 1F and 1F'). *nNOS* RNA is present in outer ectoderm of the face, excluding hatching and cement glands (Figures 1D, 1D', 1G, and 1G'). Later, *nNOS* is expressed in the head and notochord (Peunova et al., 2007). These data show that putative Kinin-Kallikrein pathway genes are simultaneously expressed in adjacent regions of the presumptive face.

### ***Putative Kinin-Kallikrein Pathway Genes Are Required for Mouth Formation and Neural Crest Development***

A requirement for *kng*, *cpn*, and *nNOS* during craniofacial development would be consistent with activity of the Kinin-Kallikrein pathway. This was tested by loss of function (LOF) using injection of morpholino antisense oligonucleotides (morpholinos, MOs) at the one-cell stage. Specificity of MO targeting was demonstrated by using two MOs, or more importantly, by “rescue” assays where a normal phenotype was observed when MO was coinjected with cognate mRNA lacking the MO target site (Figures S2A–S2D' and S2B''). For *kng* and *nNOS* MOs targeting splice sites, qPCR showed a strong decrease in endogenous RNA levels (Figures S2E and S2F). At late hatching stage (stage 40), LOF animals (“morphants”) displayed abnormal body morphology and no open mouth, with a small stomodeal invagination (Figures 2A–2D', bracket). Nostrils were absent,

eyes were small, pigment was reduced, and the face was narrow (Figures 2A'–2D'). Morphant phenotypes were apparent at early tail bud (stage 22, Figures S3A–S3L') and were accompanied by elevated cell death but normal proliferation (Figures S3M–S3V). Despite abnormal mouth phenotypes, the EAD was correctly specified as shown by expression of *frzb1* and *xanf1* (Figures 2E–2H'').

To understand LOF defects, we analyzed tail bud embryos (stage 26) for  $\beta$ -catenin indicating adherens junctions, and laminin indicating basement membrane using immunostaining. In coronal (frontal) sections, controls displayed a narrow midline strip of  $\beta$ -catenin-positive cells running from brain to cement gland, two to four cells wide (Figure 2I). However, in morphants this strip was six to eight cells wide, indicating abnormal epithelial organization (Figures 2J–2L), also apparent in parasagittal sections (Figure 2I', bracket) where morphants showed a deep region of  $\beta$ -catenin-positive tissue (Figures 2J'–2L'). In morphants, Laminin localization was largely absent from the basement membrane extending from brain to cement gland and separating epidermis and deep ectoderm (Figures 2M–2P, arrows). These data demonstrate epithelial and basement membrane abnormalities at tail bud after *kng*, *cpn*, and *nNOS* LOF.

Reduction of pigment and narrow faces in morphants suggested cranial NC may be abnormal, and, consistently, RNA expression of cranial NC markers *sox9* and *sox10* (Aoki et al., 2003; Mori-Akiyama et al., 2003) was reduced at early tail bud (stage 22) and at late tail bud (stage 26) (Figures 2Q–2X') as assayed by in situ hybridization. This was confirmed by qPCR, with >50% reduction in RNA levels (data not shown). Frontal views of control embryos at stage 26 showed a midline strip negative for NC markers (Figure 2U, bracket) that was not apparent or wider in morphants (Figure 2V–2X). These data suggest cranial NC induction, survival, proliferation, or migration is abnormal.

To assay NC induction in morphants, expression of *slug* (LaBonne and Bronner-Fraser, 1998) was examined at early neurula (stage 15) (Figures 2Y–2d). Although *nNOS* and *cpn* morphants displayed normal *slug* expression (Figures 2Y, 2Z, 2c, and 2d), *kng* morphants showed a decrease that was prevented by coinjection of *kng* mRNA (Figures 2a and 2b). Because *cpn* morphants show normal NC induction but a later deficit in NC marker expression, morphants were analyzed for alterations in proliferation and cell death. Axial sections of *sox10* in situ embryos confirmed NC identity (Figures 2e–2h). PH3 labeling demonstrated 50% reduction in mitotic cells (Figures 2i–2j and

(M–P) Parasagittal sections with laminin immunolabeling (M–P) assayed at stage 26 in two independent experiments (control morphant 100% normal, n = 10; each Kinin-Kallikrein morphant 8% normal, n = 12).  $\beta$ -catenin: green; laminin: green; nuclear propidium iodide: red. Bracket: presumptive mouth region. cg, cement gland. Scale bar, 170  $\mu$ m.

(Q–X') *kng*, *cpn*, and *nNOS* morphants showed reduced expression of neural crest markers *sox10* and *sox9*. (Q–T') *sox10* in situ hybridization at stage 22. (U–X') *sox9* in situ hybridization at stage 26. Bracket: cranial NC-free midline region. Arrow: normal extent of first arch cranial NC. Scale bars in (Q)–(X), 200  $\mu$ m; scale bars in (Q')–(T'), 800  $\mu$ m; scale bars in (U')–(X'), 400  $\mu$ m.

(Y–d) *kng* morphants showed reduced expression of *slug* at stage 22, whereas *cpn* and *nNOS* morphants and *kng* morphants coinjected with *kng* mRNA showed control *slug* levels. Arrow: specified neural crest. Dorsal view. Scale bars, 800  $\mu$ m.

(e–m) Cell proliferation and death in cranial NC cells. (e–g) *sox10* in situ hybridization at stage 22 in axial section. Control and *cpn* morpholino plus *cpn* mRNA embryos showed normal expression, whereas *cpn* morphants had reduced expression. Scale bar, 200  $\mu$ m. (h) Schematic demonstrating axial section. (i–k) Ph3 staining of axial sections show increased positive cells in control (i) relative to *cpn* morphants (j). Embryos injected with *cpn* morpholino plus *cpn* mRNA (k) had more Ph3-positive cells than *cpn* morphants. Scale bar, 170  $\mu$ m. (l and m) Quantification of Ph3 and TUNEL staining, with SD included. p value: one-way ANOVA with multiple comparisons.

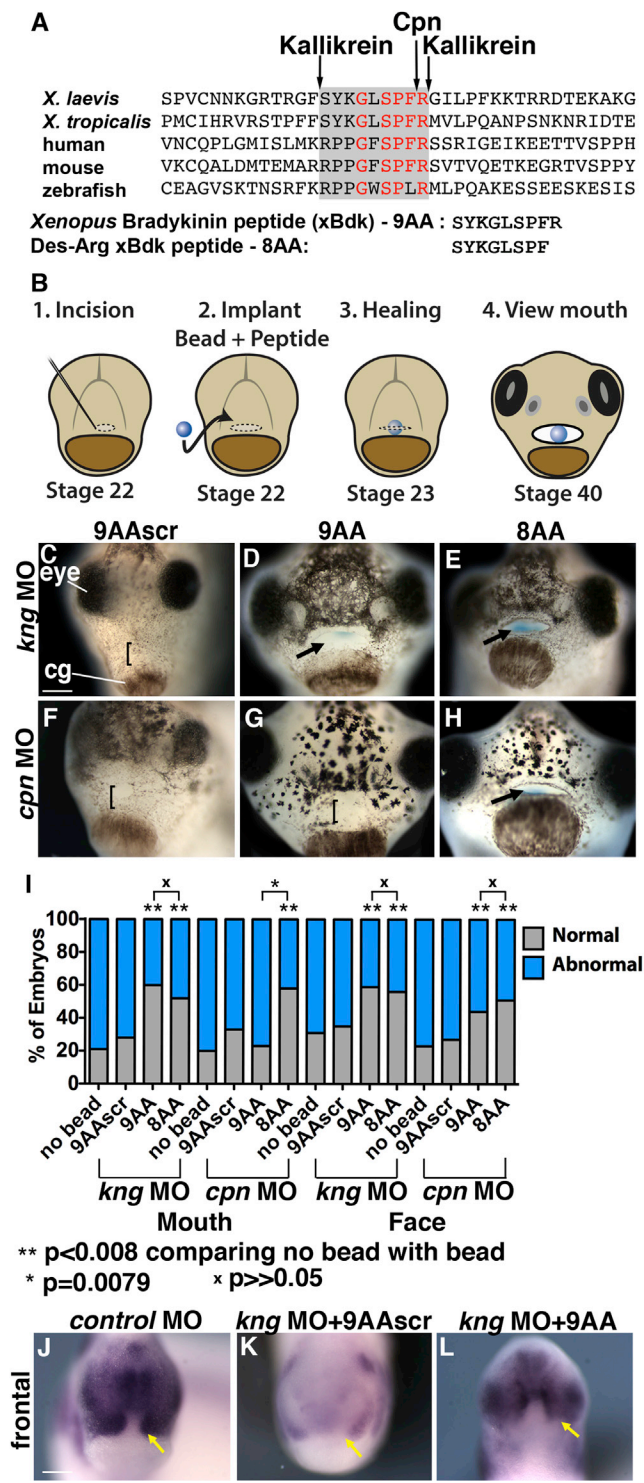


**Figure 3. Bradykinin-like Peptides Prevent *cpn* and *kng* Loss-of-Function Phenotypes**

(A) Amino acid sequence alignment of region around Bdk-I peptide. Gray highlights: Bdk-I peptide sequence; red: conserved amino acids; black arrows: Kallikrein and Cpn cleavage sites. Bdk-I (9AA) and Des-Arg Bdk-I peptides (8AA) used.

(B) Experimental design.

2l) and TUNEL demonstrated a 100% increase in dying cells in *cpn* morphants relative to controls (Figure 2m) that was partially prevented by coinjecting cognate mRNA (Figures 2k–2m). The data show a requirement for *kng*, *cpn*, and *nNOS* during craniofacial development, including mouth opening. After LOF, multiple changes are observed, in epithelial organization and NC induction, proliferation, or survival, consistent with an active embryonic Kinin-Kallikrein pathway.

***kng* and *cpn* LOF Phenotypes Are Prevented by *Xenopus* Bradykinin Peptides**

In the adult, the *Kng* precursor is processed to release a 9AA peptide, Bradykinin (Bdk) and desArg-xBdk, an 8AA peptide, after cleavage by Cpn. *Xenopus* Bdk (xBdk) peptide was predicted by aligning putative Kallikrein cleavage sites (Figure 3A) (Bor-goño et al., 2004). Considering the adult mammalian pathway, we predicted that both the 9AA and 8AA peptides should prevent the *kng* LOF phenotype, whereas only the 8AA peptide should prevent the *cpn* LOF phenotype (Figure 1A). Beads soaked in peptides were implanted medially in the future facial region of *kng* or *cpn* LOF embryos at tail bud (stage 22), which were scored at tadpole (stage 40) for mouth and facial phenotypes (Figure 3B). Relative to a scrambled xBdk peptide (Figures 3C and 3F), 9AA and 8AA peptides prevented the *kng* morphant phenotype (Figures 3D, 3E, and 3I), as predicted. In *cpn* morphants, mouth opening was restored by 8AA but not by 9AA peptide, consistent with the adult model (Figures 3G–3I). However, both peptides restored normal pigment, overall facial symmetry, and head size to *cpn* morphants (Figure 3I).

To investigate whether xBdk peptide could restore NC development after *kng* LOF, 9AA scrambled or xBdk soaked-beads were implanted medially (Figures S4J–S4L) or anterolaterally below the eye (Figures S4A–S4C') at stage 22, and *sox9* expression was later assayed. Normal *sox9* expression was observed with 9AA xBdk beads (Figures 3J–3L). Consistent data were obtained with lateral implants (Figures S4B–S4C'); however, these failed to rescue mouth formation at stage 40 (Figures S4D–S4F). These data support the hypothesis that xBdk peptides derived from *Kng* direct mouth and NC formation.

(C–H) Abnormal mouth phenotype after *kng* LOF prevented by 9AA and 8AA peptides, whereas in *cpn* morphants was prevented only by the 8AA peptide. (C) *kng* morphants implanted with 9AA scrambled (9AAscr) peptide bead (28% normal, n = 60). Embryos scored as abnormal if mouth failed to open, was tiny or asymmetric, nostrils failed to form, pigment was absent, or face was abnormally narrow. (D and E) *kng* morphant implanted with 9AA (D, 60% normal, n = 105) or 8AA bead (E, 57% normal, n = 75). (F) *cpn* morphants implanted with 9AAscr bead (mouth: 43% normal, n = 67; face: 27% normal, n = 67). (G and H) *cpn* morphants implanted with 9AA bead (mouth: 41% normal, n = 54; face: 44% normal, n = 54) or 8AA bead (mouth: 65% normal, n = 79; face: 51% normal, n = 79). Scale bar, 200  $\mu$ m.

(I) Graph depicting percent of morphants implanted with beads, displaying normal mouth and face formation. p values: one-tailed Fisher's exact test.

(J–L) Expression of neural crest marker *sox9* in *kng* morphants implanted with 9AA bead. Arrow: normal extent of first arch cranial NC. (J) Wild-type expression of *sox9* (100% normal, n = 13). *kng* morphant with a 9AAscr bead (K, 8% normal, n = 12) and 9AA bead (L, 39% normal, n = 13). Scale bar, 200  $\mu$ m.

### Nitric Oxide Prevents *kng*, *cpn*, and *nNOS* LOF Phenotypes, and Endogenous NO Production Is Regulated by xBdk

In mammals, the Kinin-Kallikrein pathway leads to production of the signaling molecule NO. We therefore hypothesized that LOF phenotypes would be prevented by application of the NO donor S-Nitroso-N-Acetyl-D,L-Penicillamine (SNAP). SNAP was coinjected with MO at the one-cell stage or injected into the face at late neurula (stage 20). When applied at the one-cell stage, SNAP prevented craniofacial and whole-body phenotypes (Figures 4A–4D'; Figures S5A–S5G, S5B'–S5D', and S5J) and corrected  $\beta$ -catenin and laminin localization and *sox9* expression (Figures 4E–4P'). When injected into the presumptive facial region, SNAP improved facial development (Figures S5A–S5D') indicating NO can act at later stages. This rescue was not due to a general effect on all MOs, because the *par1* phenotype (Ossipova et al., 2005) was not prevented by SNAP (Figures S5H–S5J). Consistent data were obtained using the NO antagonist TRIM applied at stage 20, resulting in abnormal mouth, face, and *sox9* expression (Figures 4Q–4R'). Although the Kinin-Kallikrein pathway has a role in angiogenesis (Westermann et al., 2008), craniofacial phenotypes did not result from altered blood flow, shown by a head extirpation assay. Thus, an open mouth developed in isolated heads lacking a heart and cultured from prehatching stages 31 and 32, before heartbeat until stage 41 (swimming tadpole) (Figures 4S–4T').

If NO mediates craniofacial development, it should be detectable in developing facial regions and decrease after *kng*, *cpn*, and *nNOS* LOF. NO was measured by incubating late neurula (stage 20) embryos with DAF-FM diacetate, which emits green fluorescence after reacting with NO. Tail bud (stage 26) control embryos showed fluorescence in the outer epidermis (Figure 4U), where *nNOS* is strongly expressed. Diminished fluorescence was seen and quantified in *kng*, *cpn*, and *nNOS* LOF embryos (Figures 4V–4X and 4c). *nNOS* LOF was associated with the smallest reduction in NO production, perhaps due to other NOS isoforms. We predicted that xBdk peptides would increase NO production (Figure 1A), and this was confirmed by implanting xBdk-beads into the presumptive mouth region of *kng* morphants (Figures 4Y–4c). These data demonstrate production of NO in the EAD is dependent on Kinin-Kallikrein gene function, occurs during facial development, and is responsive to xBdk.

### *cpn* Is Expressed in the EAD and Is Required Locally for Mouth Opening and Modulates Arginine Levels

Based on LOF phenotypes, we hypothesized that *kng*, *cpn*, and *nNOS* function in the EAD is locally required in the presumptive mouth and globally required for cranial NC development. This was tested by transplanting the EAD from *kng*, *cpn*, and *nNOS* LOF embryos at early tail bud (stage 22) into sibling controls (Figure 5A) (Jacox et al., 2014). Control transplants led to normal mouth opening, nostril formation, and pigmentation (Figures 5B and 5B', and quantified in Figure 5F). Strikingly, when *cpn* LOF EAD was transplanted into control embryos, open mouths or nostrils failed to form, and heads were narrow and lacked pigment, similar to global *cpn* LOF (Figures 5C and 5C'). In contrast, transplant of *nNOS* and *kng* LOF EAD into control em-

bryos led to milder phenotypes (Figures 5D–5E'), consistent with the highly preferential expression of *cpn* in the EAD, and more widespread expression of *kng* and *nNOS*. We further showed that *cpn* expression in the EAD is required for cranial NC formation because *sox9* expression at late tail bud is abnormal and reduced after EAD *cpn* LOF transplants (stage 28, Figures 5G–5H').

The activity of Cpn predicts it modulates levels of Arg (Figure 1A). To examine this, we used a quantitative assay where Arg is converted into urea whose levels can be measured (Figure 5I). As hypothesized, after *cpn* LOF, lower levels of urea relative to control embryos were present. Specificity was demonstrated as urea levels increased after injection of *cpn* mRNA into LOF embryos (Figure 5J). Together, these data indicate a requirement for Cpn activity localized in the EAD during mouth, cranial NC, and face development.

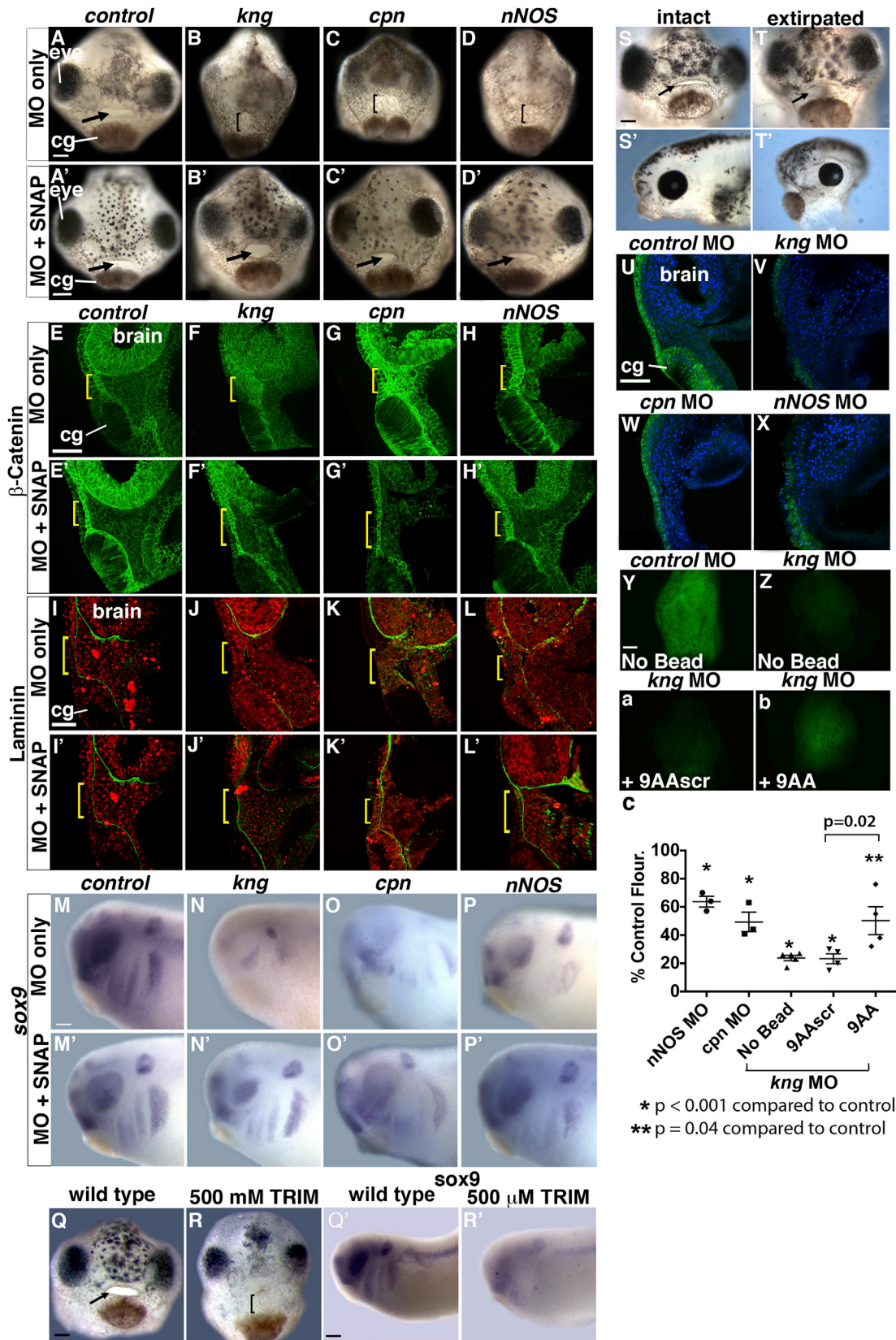
### Localized *cpn* Activity in the EAD Is Necessary for Migration of First Arch Neural Crest into the Face

The reduction in *sox9* expression with *cpn* LOF suggested that *cpn* expression is required for NC migration. To analyze migration, fluorescent cranial NC was transplanted into control or *cpn* morphant hosts at neurula (stage 18) and scored at late tail bud (stage 28) (Figure 6A). Although control transplants displayed three or four distinct branchial arches at late tail bud (stage 28) (Figures 6B and 6B'), control NC transplanted into *cpn* morphants failed to segregate into branchial arches and did not migrate (Figures 6C and 6C'), indicating a requirement for Cpn in cranial NC migration.

We extended this to ask whether local *cpn* expression is required for cranial NC migration, using double NC and EAD transplants, where control cranial NC was first transplanted into control embryos, followed by a control or *cpn* morphant EAD transplant (Figure 6D). Relative to controls (Figures 6E–E'', 6I, and 6I'), embryos with a *cpn* LOF EAD showed reduced NC migration at late tail bud (stage 28) (Figures 6F–6F'', 6J, and 6J'). In particular, first arch NC showed highly reduced migration anteriorly and medially (Figures 6J and 6J'), demonstrating that *cpn* expression in the EAD is necessary to guide the cranial NC into the face. At tadpole (stage 40), control transplants developed a normal mouth and face with extensive NC-derived tissue (Figures 6G–6G'') and a normal cartilaginous skeleton (Figures 6K and 6K'). However, *cpn* EAD LOF transplants failed to form normal mouths or faces (Figures 6H and 6H') and had substantially less NC-derived tissue (Figure 6H'') with deformed Meckel's and ceratohyal cartilages (Figures 6L and 6L'). These data demonstrate that local Cpn activity in the EAD is required for migration of the first branchial arch into the face, putatively through processing of Kng-derived peptides.

### Conservation of *kng* Function during Craniofacial Development in Zebrafish

To investigate whether the function of *kng* in face formation is conserved, we used antisense MOs to target zebrafish (*Danio*) *kng* and assayed facial cartilages in 5 day postfertilization embryos by Alcian blue staining (Figures 7A–7E' and 7F; Figures S6A–S6C' and S6D). The MOs used target the *kng1* isoform, the only transcript that includes the 9AA Bdk-I peptide. Zebrafish *kng* is expressed during NC development and mouth opening



(legend on next page)



(Figures S6E and S6F). *kng* LOF led to abnormally shaped Meckel's and ceratohyal cartilages, or abnormal spacing between Meckel's cartilage and the ethmoid plate. As in *Xenopus*, LOF led to absence of an open mouth (Figures 7G–7I). The LOF phenotype was prevented by coinjection of zebrafish *kng* that does not bind the MO (Figures 7D and 7D') or by human *KNG* RNA indicating specificity (data not shown). Morphants injected with *Xenopus laevis kng* RNA showed no rescue (Figures 7E and 7E') consistent with the greater identity between human and zebrafish Bradykinin than with *Xenopus* (Figure 3A).

Sox10::GFP transgenic fish were used to observe NC specification and migration after *kng* LOF. In both controls and morphants, NC was properly specified at the 10-somite stage (data not shown), and migration to form the first and second pharyngeal arches was normal until 48 hpf (Figures 7J–7Q'). However, by 60 hpf, Meckel's cartilage, derived from the first pharyngeal arch, fails to condense in morphants (Knight and Schilling, 2006). We conclude that zebrafish *kng* is necessary for NC and mouth development, demonstrating a conserved requirement for Kinin-Kallikrein signaling. The phenotypes observed in zebrafish are apparent at a later stage than those observed in *Xenopus*, indicating that temporal control of facial development by Kinin-Kallikrein signaling may differ between species.

## DISCUSSION

This study demonstrates activity of the Kinin-Kallikrein pathway during embryogenesis and localized control of craniofacial development through this pathway. Three major conclusions are reached. First, the embryonic pathway in *Xenopus* functions through a signaling sequence similar to that described for the adult mammalian pathway, and conservation is present in zebrafish. Second, nitric oxide (NO) production is an outcome of the pathway and is necessary for mouth and neural crest (NC) development. Third, the extreme anterior domain (EAD) functions as a

craniofacial organizer and facilitates migration of first arch cranial NC into the face via Kinin-Kallikrein signaling. These findings add insight into localized signaling essential for craniofacial development.

Epistatic relationships demonstrated for the adult pathway appear to be conserved in the embryo, such that loss of function in *kng*, *cpn*, and *nNOS* is overcome by application of the predicted peptide xBdk or by the downstream effector NO. Further, *cpn* activity and xBdk modulate levels of endogenous NO, connecting NO and Kinin-Kallikrein signaling. Consistent with a role in craniofacial signaling, pathway genes are expressed at the front of the embryo; however, their nonoverlapping expression domains suggest that initial processing of Kng to yield xBdk occurs distal to the site of xBdk processing and NO production. We did detect different sensitivity of the embryo for intact xBdk and xBdk after C-terminal Arg removal. Thus, with reduced *cpn* activity, an open mouth is formed in response only to the 8AA peptide, whereas overall face morphology is corrected by both peptides, suggesting that different downstream receptors or alternate forms of peptide processing may be available to the NC.

NO has not previously been appreciated as critical for craniofacial development. In *Xenopus*, it was proposed that NO suppresses cell proliferation and promotes convergent extension, but a facial phenotype was not explored (Peunova et al., 2007). The requirement for *kng* in zebrafish facial development implies involvement of NO, and this is in accord with effects of treating zebrafish embryos with a NO inhibitor (Kong et al., 2014). In Zebrafish, *NOS* isoforms are expressed in the developing face, specifically in the mandibular primordium and surrounding the oral cavity, consistent with this role (Poon et al., 2003, 2008). Another route to NO production is the endothelin pathway and consistent with our results, mice deficient in *endothelin-1* have craniofacial abnormalities (Kurihara et al., 1994).

### Figure 4. *kng*, *cpn*, and *nNOS* Loss-of-Function Phenotypes Are Prevented by the NO Donor, SNAP, and Kinin-Kallikrein Morphants Show Reduced Nitric Oxide Production that Is Increased by xBdk

(A–D') Facial morphology of *kng*, *cpn*, and *nNOS* loss of function (A–D) and with SNAP (A'–D'). Embryos assayed at stage 40 in three independent experiments and scored as abnormal if mouth failed to open, was tiny or asymmetric, nostrils failed to form, pigment was absent, or face was abnormally narrow. Arrow: mouth region. Bracket: unopened mouth. cg, cement gland. (A) Control MO injected (98% normal, n = 427) (B–D) *kng*, *cpn*, or *nNOS* MO injected. (A') SNAP plus control MO. (B'–D') *kng*, *cpn*, or *nNOS* MO plus SNAP coinjection (*kng* [B'] 85% normal, n = 105; *cpn* [C'] 86% normal, n = 98; *nNOS* [D'] 90% normal, n = 87). Scale bars, 100  $\mu$ m.

(E–L') Histology of *kng*, *cpn*, and *nNOS* LOF embryos after SNAP treatment. Parasagittal sections with anterior to left assayed at stage 26 with  $\beta$ -catenin (E–H') and laminin immunolabeling (I–L').  $\beta$ -catenin: green. Laminin: green, with nuclear propidium iodide: red. cg, cement gland. (E–H')  $\beta$ -catenin in control embryos (E and E'), LOF embryos (F–H), and LOF embryos coinjected with SNAP (F'–H') (*kng* [F'] 100% normal, n = 5; *cpn* [G'] 100% normal, n = 5; *nNOS* [H'] 100% normal, n = 5). (I–L') Laminin staining in control embryos (I and I'), LOF embryos (J–L), and LOF embryos coinjected with SNAP (J'–L') (*kng* [J'] 75% normal, n = 4; *cpn* [K'] 80% normal, n = 5; *nNOS* [L'] 100% normal, n = 4). Scale bars, 170  $\mu$ m.

(M–P') Expression of *sox9* RNA (in situ hybridization) after SNAP injection into *kng* (N, N'), *cpn* (O, O'), and *nNOS* (P, P') LOF embryos. Lateral view. Scale bar, 100  $\mu$ m. (Q–R') NOS inhibitor TRIM prevents mouth formation and reduces *sox9* expression. (Q and Q') Wild-type embryos (100% normal, n = 6). (R and R') TRIM-treated embryos (17% normal, n = 6). (Q and R) Frontal view at stage 40. (Q' and R') Lateral view of *sox9* in situ hybridization at stage 26. Scale bars in (Q) and (R), 100  $\mu$ m; scale bars in (Q') and (R'), 400  $\mu$ m.

(S–T') Extirpated heads show open mouth and normal pigmentation at swimming tadpole (stage 41). (S and S') Control heads (96% normal, n = 27). (T and T') Isolated heads (92% normal, n = 26). (S and T) frontal view. (S' and T') side view. Scale bar, 100  $\mu$ m.

(U–X) Fluorescence after incubation with NO sensor DAF-FM in control embryos (U), *kng* (V), *cpn* (W), and *nNOS* (X) LOF embryos. cg, cement gland. Sagittal view. Scale bar, 170  $\mu$ m.

(Y–c) Control morphant with no bead (Y). *kng* morphant with no bead (Z), with 9AA xBdk scrambled bead (a) or 9AA xBdk bead (b). Images collected with same exposure, gain, and fluorescent illumination. *kng* morphants implanted with 9AA xBdk bead displayed 50% of control fluorescence compared with 23% of control fluorescence in morphants treated with 9AAscr xBdk peptide. Frontal view. Scale bar, 100  $\mu$ m. (c) Graph showing morphant fluorescence as percentage of control fluorescence; *cpn* morphants: 49%, *kng* morphants: 24%, and *nNOS* morphants: 64%. Each dot represents average of three biological replicates from independent experiments. p values: one-tailed t test.

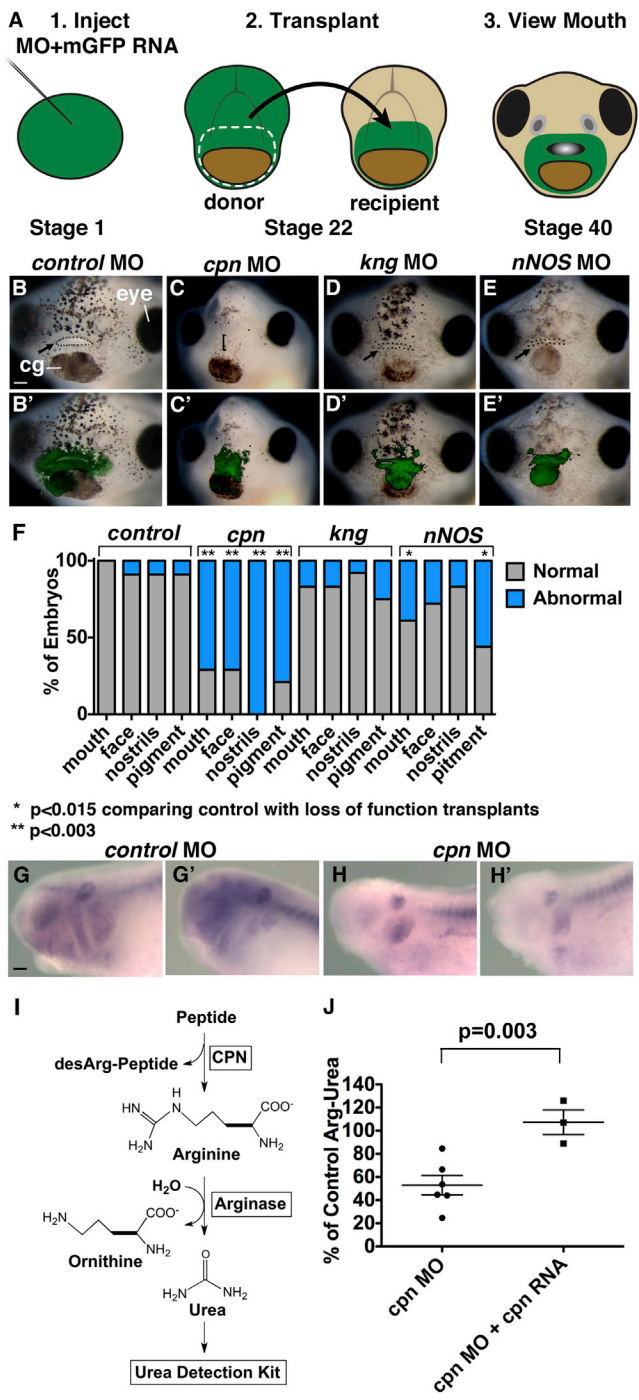


**Figure 5. Local *cpn* Expression Is Required for Mouth Opening**

Local requirement of *kng*, *cpn*, and *nNOS* expression tested with EAD transplants.

(A) Experimental design: donor morphant tissue was transplanted to uninjected sibling recipients.

(B–E') EAD transplant outcome from control, *cpn*, *kng*, or *nNOS* morphant donor tissue (control [B] 100% normal, n = 11; *cpn* [C] 28% normal, n = 14; *kng* [D] 83% normal, n = 24; *nNOS* [E] 61% normal mouth phenotype, 72% normal facial phenotype, n = 18). (B'–E') Overlay of (B)–(E) with GFP fluorescence indicating donor tissue. Dots surround open mouths. Bracket: unopened mouth. Frontal view. Scale bar, 100  $\mu$ m.

The demonstration that the EAD is necessary for migration of the first arch NC into the facial region addresses the long-standing question of what region might guide the migratory cranial NC into the face. Our findings not only underscore the organizer capacity of the EAD, but identify *cpn* locally expressed in the EAD as required for NC ingress, possibly through processing of Kng-derived peptides. Consistent with a guidance function for xBdk, midline or lateral placement (into the EAD) of xBdk-impregnated beads was sufficient to overcome the NC migration defect after Kinin-Kallikrein LOF. Bradykinin is promigratory in other settings, for malignant cells and trophoblasts, whereas NO is involved in inflammation-induced cell migration (Chen et al., 2000; Cuddapah et al., 2013; Erices et al., 2011; Yu et al., 2013). Interestingly, another substrate for CPN is C3a, a small complement peptide required for more local aspects of cranial NC migration (Carmona-Fontaine et al., 2011; Matthews et al., 2004).

In addition to a role for Kinin-Kallikrein signaling in NC migration, *kng* is necessary for NC induction, whereas *cpn* is needed later for NC proliferation and survival, highlighting complex spatiotemporal requirements for Kinin-Kallikrein signaling during NC development. Unlike NC specification, mouth specification does not depend on Kinin-Kallikrein signaling. However, mouth opening is tightly linked to NC that abuts the EAD, suggesting that the Kinin-Kallikrein pathway may indirectly regulate mouth opening through the NC. Consistently, application of a xBdk peptide or NO donor after mouth specification and neural tube closure restored a normal NC, normal face morphology, and concomitantly an open mouth to LOF embryos.

Genes that encode Kinin-Kallikrein pathway factors are found in all vertebrates, raising the question of whether activity of this pathway during craniofacial development is conserved. The requirement for *kng* function during zebrafish NC development and mouth formation supports broad conservation. Additionally, ACE inhibitors that stabilize Bradykinin, used to treat high blood pressure, are teratogens associated with human craniofacial defects (Barr and Cohen 1991). In mammals, single-gene LOF in Kinin-Kallikrein pathway proteins do not obviously result in craniofacial defects (Cheung et al., 1993; Mashimo and Goyal, 1999; Merkulov et al., 2008; Mueller-Ortiz et al., 2009); however, certain double mutants or compound heterozygotes have not been examined. Humans heterozygous for CPN function suffer from angioedema without developmental manifestation; however, no reported patients have complete CPN deficiency, indicating an essential function for this protein (Matthews et al., 2004). A screen for mouse genes involved in craniofacial

(F) Quantification of structure depending on morphant background of facial tissue.

(G–H') *sox9* expression in *cpn* morphant donor tissue transplants, compared with control morphant transplants. *sox9* in situ hybridization in control morphant transplants (G, G', 70% with normal expression, n = 10) and *cpn* morphant transplants (H and H', 36% with normal expression, n = 11). Two representative embryos shown. Scale bar, 100  $\mu$ m.

(I and J) (I) Summary of urea assay for analysis of Cpn activity. (J) Chart summarizing level of urea derived from free Arg in *cpn* morphants or morphants coinjected with *cpn* RNA, as percent of urea derived from free Arg in control morphants. Urea levels in control morphants and wild-type embryos were equivalent. Each dot represents an independent experiment. p value: one-tailed t test.

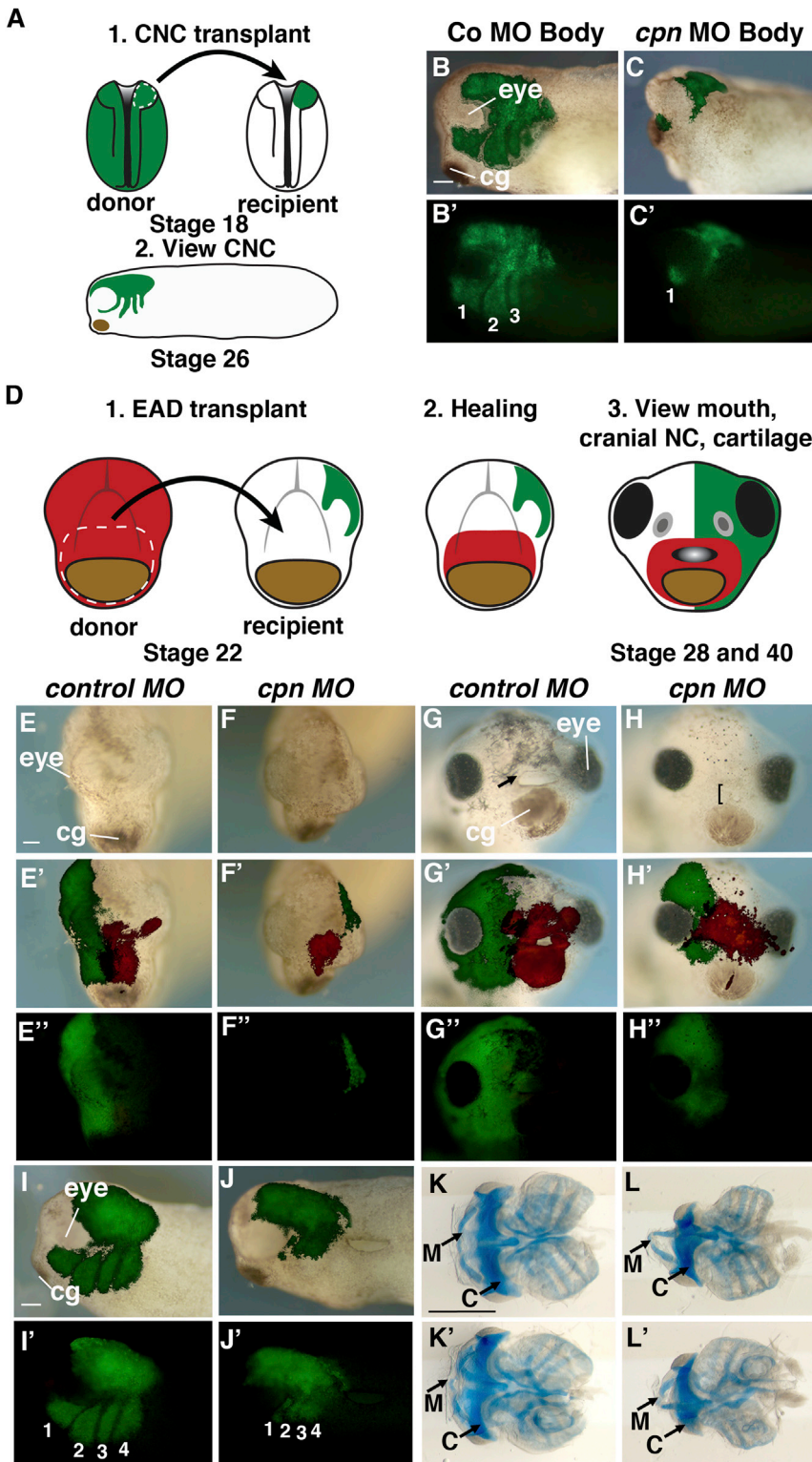


**Figure 6. Global and local *cpn* Expression Is Required for Cranial Neural Crest Migration**

Global requirement for *cpn* expression tested with cranial NC transplants. Embryos scored as normal if three or four distinct branchial arches formed and migrated normally.

(A) Experimental design: donor wild-type cranial NC transplanted into *cpn* morphant sibling recipients.

(B–C') (B and C) Cranial NC transplant outcomes in control and *cpn* morphant recipients with GFP fluorescence overlay, indicating location of donor transplant at stage 28 (control [B] 69% normal, n = 36; *cpn* [C] 27% normal, n = 29). (B' and C') GFP fluorescence of cranial NC in control and *cpn* morphant recipient. Numbers indicate branchial arches. Side view. cg, cement gland. Scale bar, 200  $\mu$ m.

(D) Experimental design: donor *cpn* morphant EAD transplanted into control morphant sibling recipients with fluorescent cranial NC.

(E–H'') (E, F, G, and H) Bright-field view of control and *cpn* morphant transplants at stages 28 and 40. (E', F', G', and H') Cranial NC in control and *cpn* morphant EAD recipients at stages 28 and 40 with GFP fluorescence overlay, indicating location of cranial NC and mCherry fluorescence overlay, indicating location of EAD transplant. (control stage 28 [E'] 85% normal, n = 41; *cpn* stage 28 [F'] 57% normal, n = 42; control stage 40 [G'] 63% normal, n = 38; *cpn* stage 40 [H'] 17% normal, n = 35). (E'', F'', G'', and H'') GFP fluorescence of cranial NC in control and *cpn* morphant EAD recipients at stage 28 and 40. Arrow: Open mouth. Bracket: unopened mouth. Frontal view. cg, cement gland. Scale bar, 100  $\mu$ m.

(I–J') (I and J) Cranial NC outcome in control and *cpn* morphant EAD recipients with GFP fluorescence overlay, indicating location of cranial NC at stage 28. (I' and J') GFP fluorescence of cranial NC in control and *cpn* morphant EAD recipients. Numbers indicate branchial arches. Side view. cg, cement gland. Scale bar, 200  $\mu$ m.

(K–L') Cartilage in control morphant EAD recipients (K, K' 78% normal, n = 14) and *cpn* morphant EAD recipients (L, L' 6% normal, n = 16). (K and L) Ventral view. (K' and L') Dorsal view. M, Meckel's cartilage. C, ceratohyal cartilage. Scale bar, 100  $\mu$ m.

2003). It is also possible that redundant genes or another pathway such as endothelin signaling work together with Kinin-Kallikrein signaling.

Our study defines the Kinin-Kallikrein pathway and nitric oxide as key for craniofacial development in *Xenopus* and zebrafish and addresses the long-standing question of how the NC specif-

ically moves into the face. The observations suggest important future directions, including mechanistic studies addressing a putative NC guidance function for xBdk and other EAD-derived

development identified a Glutamate Carboxypeptidase and a Protein Inhibitor of Nitric Oxide (PIN), suggesting that NO activity is involved in mammalian facial development (Fowles et al.,

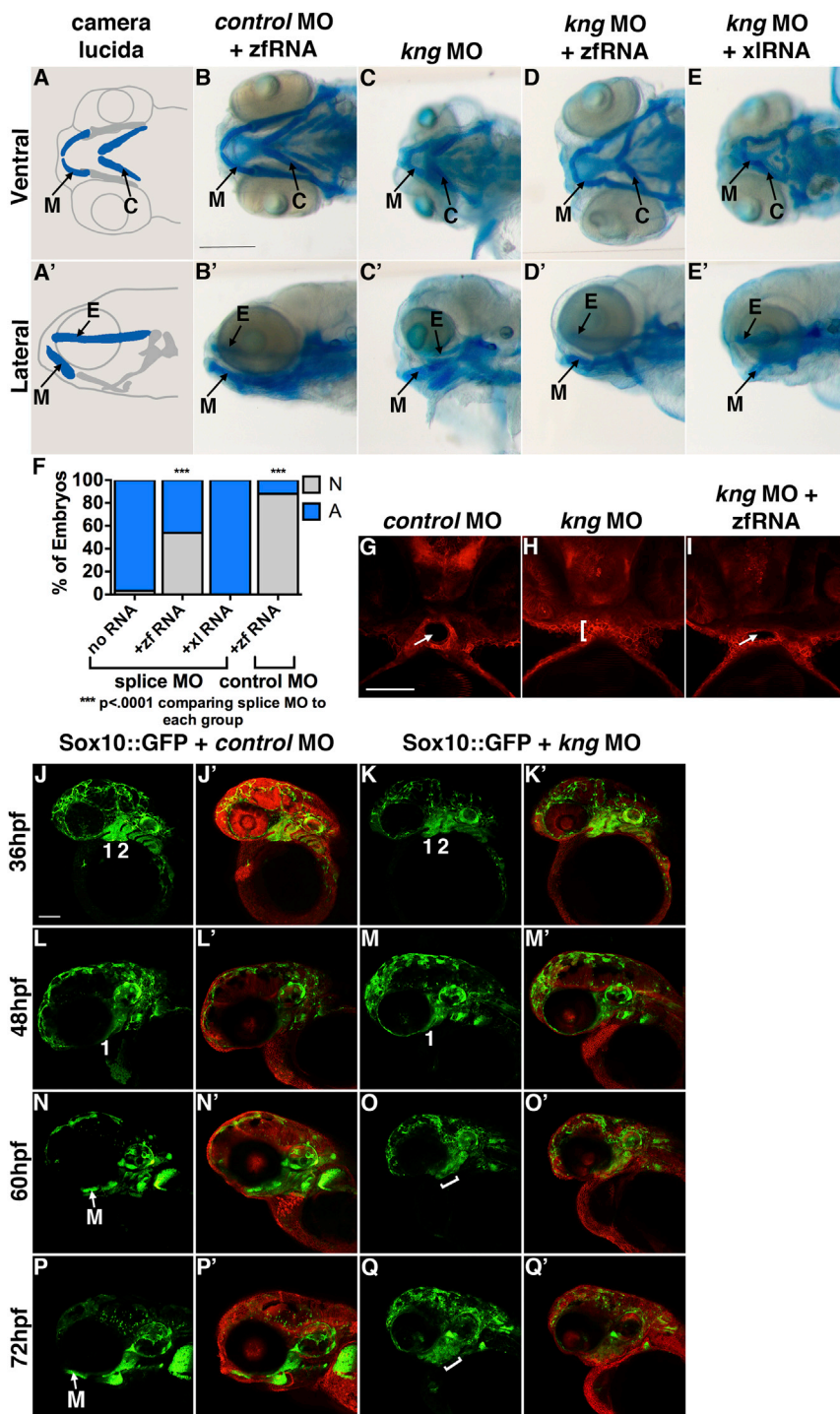


**Figure 7. Function of *kng* in Craniofacial Development Is Conserved in Zebrafish**

(A and A') Camera lucida of facial cartilages. E, ethmoid plate; C, ceratohyal cartilage; M, Meckel's cartilage.

(B–E') *kng* loss of function using splice morpholinos and rescue with zebrafish (*zf*) *kng* mRNA. Embryonic cartilage scored at 5 dpf after Alcian blue staining in three independent experiments. Scale bar, 250  $\mu$ m. (B and B') Control morphants coinjected with mRNA were normal (88% normal, n = 50). (C, C', E, and E') *kng* morphants and *kng* morphants coinjected with 200 ng *Xenopus kng* mRNA showed abnormal facial cartilage. Meckel's cartilage was truncated, boxy, and pointed at an abnormal angle. The ceratohyal cartilage was positioned at an abnormal angle, perpendicular to the midline. (*kng* [C and C'] 3% normal, n = 61; *kng* mo plus frog mRNA [E and E'] 0% normal, n = 65). (D and D') *kng* morphants coinjected with 200 ng zebrafish (*zf*) mRNA showed partial rescue. Embryos scored as partially rescued if Meckel's cartilage was longer, more rounded, and pointed dorsally and if ceratohyal cartilage pointed more anteriorly, compared to *kng* morphants (54% partial rescue, n = 89).

(F) Quantification of phenotypes. p values: one-tailed Fisher's exact test. N, normal or partially rescued phenotype. A, abnormal phenotype.

(G–I) Ventral views of mApple-injected embryos at 48 hpf. White arrow: open mouth. White bracket: closed mouth. Scale bar, 100  $\mu$ m. (G) Control morphants (100% normal, n = 5). (H) *kng* splice morphants failed to form open mouths (0% normal, n = 6). (I) *kng* splice morphants coinjected with 200 ng *zf* mRNA had open mouths (67% normal, n = 6).

(J–Q') Confocal images of Sox10::GFP zebrafish coinjected with 75 pg mApple and 4 ng control morpholino (100% normal, n = 5) or 4 ng *kng* splice morpholino (0% normal, n = 5). Paired images of the same embryo show GFP signal alone and GFP with mApple. Numbers indicate pharyngeal arches (PA). Bracket: uncondensed/disorganized cartilage. Lateral view. M, Meckel's cartilage. Scale bar, 100  $\mu$ m. (J–K') At 36 hpf, NC has migrated into the face of both morphant and control embryos to form first and second PA. (L–M') At 48 hpf, the first PA has begun to extend under eye to form the lower jaw in both morphant and control embryos. (N and N') At 60 hpf, first PA has condensed into Meckel's cartilage in control embryos. (O and O') At 60 hpf, first PA remains disorganized in morphants and does not condense. (P and P') At 72 hpf, Meckel's cartilage is prominent in control embryos. (Q and Q') At 72 hpf, cartilage of the lower jaw remains disorganized and uncondensed in morphants.

activities, and the relationship between NC migration and mouth formation.

## EXPERIMENTAL PROCEDURES

### Embryo Preparation

*Xenopus laevis* and zebrafish, *Danio rerio* embryos were cultured using standard methods (Sive et al., 2000; Westerfield et al., 2001). *Xenopus* embryos

were staged according to Nieuwkoop and Faber (1994); *Danio* embryos were staged according to Kimmel et al. (1995). Lines used were Sox10::GFP (Curtin et al., 2011). All animal use is reviewed and approved by MIT IACUC, under protocol number 0414-026-17.

### RNA and qPCR

RNA extraction, cDNA preparation, and qPCR measurements were conducted according to Dickinson and Sive (2009). Primer sequences are available on

request. Three sets of five heads at stage 22 for *sox10* and at stage 26 for *sox9* were collected for each of four conditions, including control MO, *cpn* MO, *kng* MO, and *nNOS* MO to provide biological replicates. Equal amounts of RNA were used for reverse transcription (RT) and qPCR to measure *sox9* or *sox10* RNA. qPCR data from three readings for each of four conditions were averaged, and their distribution was plotted to determine SD. Average morphant qPCR value divided by control morphant qPCR value gave expression level relative to control.

### In Situ Hybridization

cDNA sequences used to transcribe in situ hybridization probes including *cpn* (BC059995), *kng* (BC083002), *nNOS* (Peunova et al., 2007), *sox9* (AY035397), *sox10* (Aoki et al., 2003), *xanf1* (Ermakova et al., 2007), *frzb1* (BC108885), and XCG (Sive et al., 1989). In situ hybridization was performed as described by Sive et al. (2000), without proteinase K treatment. Double-staining protocol adapted from Wiellette and Sive (2003).

### Morpholinos and RNA Rescues

*Xenopus* antisense morpholino-modified oligonucleotides (morpholinos [MOs]) included one start site MO targeting *cpn*, two splice site MOs against *kng* and *nNOS*, and a standard control MO. Sequences are as follows: *cpn* MO 5'-ACCACAATCCCAGTGCCATTCTCCC-3', *kng* MO 5'-TTTTACCCATTGTCTTACCTGTC-3', *nNOS* MO 5'-TGGCTAAAAGAACACAGGACATCAA-3'. *nNOS* MO resulted in an intron inclusion with an early stop codon at AA313, whereas *kng* MO resulted in an aberrant transcript that could not be amplified by RT-PCR, suggesting it was too large to be amplified or the primer binding sites spanning the MO sequence were missing. qPCR in Figure S2E confirms a reduction in normal *kng* mRNA transcript following MO treatment. *Danio* morpholinos include a start site and a splice site MO targeting *kng1*. Sequences are *kng1* MO (5'-CAAGCTCTTGCCAGCGCCATTGTC-3') and *kng1* MO (5'-AGCCTGAGGAAACACAAACGCACGT-3'). The splice site *kng1* morpholino binds the terminal 22 bp of intron 2 and the first 3 bp of exon 3.

*kng* cDNA, *nNOS* cDNA, and *cpn* cDNA without 5' UTRs were cloned into the CS2<sup>+</sup> vector. RNA was generated in vitro using the mMESSAGE mMACHINE kit (Ambion). RNA (~1 ng) and morpholino (14–18 ng) were coinjected at the one-cell stage to test morpholino specificity via RNA rescue.

### Peptide and NO Donor Rescues

Peptides (Thermo Scientific) were designed according to predicted sequences including 9 amino acid (AA) *Xenopus* Bradykinin (xBdk) (SYKGLSPFR) and 8AA Des-Arg xBdk (SYKGLSPF) and diluted to 0.1 or 0.2 mg/ml. Affi-gel blue agarose beads (50–100 mesh, Bio-Rad) loaded with peptides were prepared according to Carmona-Fontaine (2011). For rescues, beads resuspended in 0.1 mg/ml peptide solution were implanted in the presumptive mouth region at stage 22 and scored at stage 40. For NC assays, beads resuspended in 0.2 mg/ml peptide solution were implanted in the side of the head or presumptive mouth at stages 20–22. Embryos were fixed at tail bud (stage 26) for in situ hybridization analysis. For peptide-rescue assays, partial LOF morphants were employed to maximize viability.

NO donor, S-Nitroso-N-acetyl-DL-penicillamine (SNAP) (Sigma) was diluted to 100 mM in a 50% DMSO solution. For early rescues, 1 nl of SNAP was co-injected with 17 ng of morpholino into one-cell stage embryos. For late rescues (stage 20), 2–3 nl of SNAP was injected into the presumptive mouth region. The *nNOS* inhibitor, TRIM (Sigma, T7313), was diluted to 1 M concentration in DMSO and applied to late neurula (stage 20) embryos. Embryos were collected at tail bud (stage 26) for *sox9* in situ hybridization and at swimming tadpole (stage 40) for craniofacial morphology.

### Nitric Oxide Staining and Quantification

Embryos were incubated in NO indicator 4-amino-5-methylamino-2',7'-difluorofluorescein diacetate (1:150), (DAF-FM diacetate; Invitrogen; Lepiller et al., 2007) for 2–3 hr at 26°C. Embryos were fixed in 4% paraformaldehyde overnight, embedded in 4% agarose, vibratome sectioned (100  $\mu$ m), counterstained with DAPI, and imaged on a Zeiss LSM 700 Laser Scanning Confocal. For NO quantification, 120 embryos per condition were decapitated, washed, dounced, and spun (10 min, 1,300 rpm). The clear fraction was divided in triplicate and loaded on a microplate (Corning 3993- half-area, flat bottom, black),

and fluorescence was measured using a Teican microplate reader. Untreated head solution was used to measure background fluorescence

### Urea Assay

A bovine Arginase solution (2 mg/ml lyophilized bovine Arginase [Sigma # A3233] in 50 mM MnCl<sub>2</sub>) was incubated for 1 hr at 37°C. Stage 28–29 embryos were anesthetized and decapitated, with 180 heads per condition. Heads were dounced in 90  $\mu$ l of water, spun for 10 min at 1,100 rpm at 4°C, and 100  $\mu$ l of clear, cytoplasmic fraction was mixed with 75  $\mu$ l of Arginase solution for a 2 hr incubation at 37°C. Urea content was detected using the Abcam Urea Assay Kit (Abcam #AB83362). Absorbance was read on a Teican "Infinite Pro" microplate reader and calculated as a percentage of wild-type or control morphant level.

### Immunohistochemistry

Immunohistochemistry was performed as described (Dickinson and Sive, 2006). Primary antibodies included polyclonal anti-laminin antibody (Sigma L-9393) diluted 1:150 and polyclonal anti- $\beta$ -catenin (Invitrogen) diluted 1:100. Secondary antibody was Alexa 488 goat anti-rabbit (Molecular Probes) diluted 1:500 with 0.1% propidium iodide as a counterstain. Sections were imaged on Zeiss LSM 700 and 710 Laser Scanning Confocal microscopes. Images were analyzed using Imapis (Bitplane) and Photoshop (Adobe).

### Whole-Mount TUNEL, PH3, and Alcian Blue Labeling

TUNEL and PH3 labeling were performed according to Dickinson and Sive (2006, 2009). Alcian blue staining was performed according to Kennedy and Dickinson (2012).

### Transplants and Head Extirpation

EAD transplants were performed according to Jacox et al. (2014); NC transplants were performed according to Mancilla and Mayor (1996). For head extirpation, morphant and wild-type embryos were grown to stage 31–32, when the stomodeum forms. Embryos were anesthetized in Tricaine, and heads were removed below the cement gland excluding the developing heart. Heads were moved to 0.5  $\times$  modified Barth's saline for healing and growth. Whole embryos and heads were scored for facial and mouth development at stage 40.

### SUPPLEMENTAL INFORMATION

Supplemental Information includes six figures and can be found with this article online at <http://dx.doi.org/10.1016/j.celrep.2014.06.026>.

### AUTHOR CONTRIBUTIONS

L.J. designed and conducted all bead, extirpation, transplant, migration LOF and rescue assays (Figures 3, 4S–4T, 5, and 6), NO and urea quantification assays (Figures 4Y–4c, and 5I–5J), and in situ hybridization experiments (Figures 2Q–2g, 3J–3L, and 5G–5H'). L.J. wrote and revised the manuscript drafts. R.S. designed and tested morpholinos, executed LOF rescues with cognate RNA and SNAP, and conducted immunohistochemistry and NO staining (Figures 2A–2D', 2I–2P, 4A–4L', 4Q–R', and 4U–4X), except for Ph3 and TUNEL experiments, conducted by L.J. (Figures 2h–2l). R.S. contributed in situ hybridization data (Figures 4M–4P' and 2E–2H'') and obtained or cloned all plasmids. R.S. and L.J. assembled and modified figures and contributed in situ hybridization data shown in Figure 1. J.C. designed and conducted all experiments in zebrafish (Figures 7 and S6) and contributed to manuscript preparation. A.R. contributed in situ hybridization data (Figures 2Y–2Z and 2a–2g). A.D. identified CPN and kininogen in the EAD and performed initial experiments. H.S. directed and supervised the study and wrote the manuscript.

### ACKNOWLEDGMENTS

We thank Cas Bresilla for frog husbandry, our colleagues for discussion and critical input, especially Jasmine McCammon and Ryann Fame. Thanks to George Bell for help with bioinformatics, Nicki Watson and Wendy Salmon

for imaging support, and Tom diCesare for assistance with graphics. We thank Eric Liao for his gift of Sox10::GFP fish, for collegial discussion and for communicating results prior to publication. Thanks to Natalia Peunova, Andrey Zaraisky, and Jean-Pierre Saint-Jeannet for gifts of plasmids. We are grateful to the NIDCR for support (1R01 DE021109-01 to H.S. and F30DE022989 to L.J.), Harvard University for the Herschel Smith Graduate Fellowship (to L.J.), and the American Association of Anatomists (for a postdoctoral fellowship to R.S.).

Received: November 10, 2013

Revised: April 24, 2014

Accepted: June 17, 2014

Published: July 17, 2014

## REFERENCES

- Aoki, Y., Saint-Germain, N., Gyda, M., Magner-Fink, E., Lee, Y.H., Credidio, C., and Saint-Jeannet, J.P. (2003). Sox10 regulates the development of neural crest-derived melanocytes in *Xenopus*. *Dev. Biol.* *259*, 19–33.
- Barr, M., Jr., and Cohen, M.M., Jr. (1991). ACE inhibitor fetopathy and hypocalvaria: the kidney-skull connection. *Teratology* *44*, 485–495.
- Borgoño, C.A., Michael, I.P., and Diamandis, E.P. (2004). Human tissue kallikreins: physiologic roles and applications in cancer. *Mol. Cancer Res.* *2*, 257–280.
- Bradley, S., Tossell, K., Lockley, R., and McDearmid, J.R. (2010). Nitric oxide synthase regulates morphogenesis of zebrafish spinal cord motoneurons. *J. Neurosci.* *30*, 16818–16831.
- Bryant, J.W., and Shariat-Madar, Z. (2009). Human plasma kallikrein-kinin system: physiological and biochemical parameters. *Cardiovasc. Hematol. Agents Med. Chem.* *7*, 234–250.
- Carmona-Fontaine, C. (2011). PhD Thesis. University College of London. Epub. <http://carloscarmonafontaine.wikispaces.com/Thesis>
- Carmona-Fontaine, C., Thevenneau, E., Tzekou, A., Tada, M., Woods, M., Page, K.M., Parsons, M., Lambris, J.D., and Mayor, R. (2011). Complement fragment C3a controls mutual cell attraction during collective cell migration. *Dev. Cell* *21*, 1026–1037.
- Chang, A.C., Fu, Y., Garside, V.C., Niessen, K., Chang, L., Fuller, M., Setiadi, A., Smrz, J., Kyle, A., Minchinton, A., et al. (2011). Notch initiates the endothelial-to-mesenchymal transition in the atrioventricular canal through autocrine activation of soluble guanylyl cyclase. *Dev. Cell* *21*, 288–300.
- Chen, A., Kumar, S.M., Sahley, C.L., and Muller, K.J. (2000). Nitric oxide influences injury-induced microglial migration and accumulation in the leech CNS. *J. Neurosci.* *20*, 1036–1043.
- Cheung, P.P., Kunapuli, S.P., Scott, C.F., Wachtfogel, Y.T., and Colman, R.W. (1993). Genetic basis of total kininogen deficiency in Williams' trait. *J. Biol. Chem.* *268*, 23361–23365.
- Contestabile, A., and Ciani, E. (2004). Role of nitric oxide in the regulation of neuronal proliferation, survival and differentiation. *Neurochem. Int.* *45*, 903–914.
- Cooke, J.P. (2003). NO and angiogenesis. *Atheroscler. Suppl.* *4*, 53–60.
- Cuddapah, V.A., Turner, K.L., Seifert, S., and Sontheimer, H. (2013). Bradykinin-induced chemotaxis of human gliomas requires the activation of KCa3.1 and ClC-3. *J. Neurosci.* *33*, 1427–1440.
- Curtin, E., Hickey, G., Kamel, G., Davidson, A.J., and Liao, E.C. (2011). Zebrafish *wnt9a* is expressed in pharyngeal ectoderm and is required for palate and lower jaw development. *Mech. Dev.* *128*, 104–115.
- Dickinson, A.J., and Sive, H. (2006). Development of the primary mouth in *Xenopus laevis*. *Dev. Biol.* *295*, 700–713.
- Dickinson, A., and Sive, H. (2007). Positioning the extreme anterior in *Xenopus*: cement gland, primary mouth and anterior pituitary. *Semin. Cell Dev. Biol.* *18*, 525–533.
- Dickinson, A.J., and Sive, H.L. (2009). The Wnt antagonists Frzb-1 and Crescent locally regulate basement membrane dissolution in the developing primary mouth. *Development* *136*, 1071–1081.
- Erices, R., Corthorn, J., Lisboa, F., and Valdés, G. (2011). Bradykinin promotes migration and invasion of human immortalized trophoblasts. *Reprod. Biol. Endocrinol.* *9*, 97.
- Ermakova, G.V., Solovieva, E.A., Martynova, N.Y., and Zaraisky, A.G. (2007). The homeodomain factor Xanf represses expression of genes in the presumptive rostral forebrain that specify more caudal brain regions. *Dev. Biol.* *307*, 483–497.
- Filippin, L.I., Cuevas, M.J., Lima, E., Marroni, N.P., Gonzalez-Gallego, J., and Xavier, R.M. (2011). Nitric oxide regulates the repair of injured skeletal muscle. *Nitric Oxide* *24*, 43–49.
- Fowles, L.F., Bennetts, J.S., Berkman, J.L., Williams, E., Koopman, P., Teasdale, R.D., and Wicking, C. (2003). Genomic screen for genes involved in mammalian craniofacial development. *Genesis* *35*, 73–87.
- Jacox, L.A., Dickinson, A.J., and Sive, H. (2014). Facial transplants in *Xenopus laevis* embryos. *J. Vis. Exp.* (85).
- Jeseta, M., Marin, M., Tichovska, H., Melicharova, P., Cailliau-Maggio, K., Martoriati, A., Lescuyer-Rousseau, A., Beaujois, R., Petr, J., Sedmikova, M., and Bodart, J.F. (2012). Nitric oxide-donor SNAP induces *Xenopus* eggs activation. *PLoS ONE* *7*, e41509.
- Kakoki, M., and Smithies, O. (2009). The kallikrein-kinin system in health and in diseases of the kidney. *Kidney Int.* *75*, 1019–1030.
- Kennedy, A.E., and Dickinson, A.J. (2012). Median facial clefts in *Xenopus laevis*: roles of retinoic acid signaling and homeobox genes. *Dev. Biol.* *365*, 229–240.
- Kimmel, C.B., Ballard, W.W., Kimmel, S.R., Ullmann, B., and Schilling, T.F. (1995). Stages of embryonic development of the zebrafish. *Dev. Dyn.* *203*, 253–310.
- Knight, R.D., and Schilling, T.F. (2006). Cranial neural crest and development of the head skeleton. *Adv. Exp. Med. Biol.* *589*, 120–133.
- Kong, Y., Grimaldi, M., Curtin, E., Dougherty, M., Kaufman, C., White, R.M., Zon, L.I., and Liao, E.C. (2014). Neural crest development and craniofacial morphogenesis is coordinated by nitric oxide and histone acetylation. *Chem. Biol.* *21*, 488–501.
- Kurihara, Y., Kurihara, H., Suzuki, H., Kodama, T., Maemura, K., Nagai, R., Oda, H., Kuwaki, T., Cao, W.H., Kamada, N., et al. (1994). Elevated blood pressure and craniofacial abnormalities in mice deficient in endothelin-1. *Nature* *368*, 703–710.
- Kuzin, B., Roberts, I., Peunova, N., and Enikolopov, G. (1996). Nitric oxide regulates cell proliferation during *Drosophila* development. *Cell* *87*, 639–649.
- LaBonne, C., and Bronner-Fraser, M. (1998). Neural crest induction in *Xenopus*: evidence for a two-signal model. *Development* *125*, 2403–2414.
- Lepiller, S., Laurens, V., Bouchot, A., Herbomel, P., Solary, E., and Chluba, J. (2007). Imaging of nitric oxide in a living vertebrate using a diamino-fluorescein probe. *Free Radic. Biol. Med.* *43*, 619–627.
- Mancilla, A., and Mayor, R. (1996). Neural crest formation in *Xenopus laevis*: mechanisms of Xslug induction. *Dev. Biol.* *177*, 580–589.
- Mashimo, H., and Goyal, R.K. (1999). Lessons from genetically engineered animal models. IV. Nitric oxide synthase gene knockout mice. *Am. J. Physiol.* *277*, G745–G750.
- Matthews, K.W., Mueller-Ortiz, S.L., and Wetsel, R.A. (2004). Carboxypeptidase N: a pleiotropic regulator of inflammation. *Mol. Immunol.* *40*, 785–793.
- Mayor, R., and Thevenneau, E. (2013). The neural crest. *Development* *140*, 2247–2251.
- McLean, D.L., and Sillar, K.T. (2000). The distribution of NADPH-diaphorase-labelled interneurons and the role of nitric oxide in the swimming system of *Xenopus laevis* larvae. *J. Exp. Biol.* *203*, 705–713.
- Merkulov, S., Zhang, W.M., Komar, A.A., Schmaier, A.H., Barnes, E., Zhou, Y., Lu, X., Iwaki, T., Castellino, F.J., Luo, G., and McCrae, K.R. (2008). Deletion of murine kininogen gene 1 (mKng1) causes loss of plasma kininogen and delays thrombosis. *Blood* *111*, 1274–1281.
- Moncada, S., and Higgs, E.A. (1995). Molecular mechanisms and therapeutic strategies related to nitric oxide. *FASEB J.* *9*, 1319–1330.

- Mori-Akiyama, Y., Akiyama, H., Rowitch, D.H., and de Crombrughe, B. (2003). Sox9 is required for determination of the chondrogenic cell lineage in the cranial neural crest. *Proc. Natl. Acad. Sci. USA* *100*, 9360–9365.
- Mueller-Ortiz, S.L., Wang, D., Morales, J.E., Li, L., Chang, J.Y., and Wetsel, R.A. (2009). Targeted disruption of the gene encoding the murine small subunit of carboxypeptidase N (CPN1) causes susceptibility to C5a anaphylatoxin-mediated shock. *J. Immunol.* *182*, 6533–6539.
- Nieuwkoop, P.D., and Faber, J. (1994). Normal table of *Xenopus laevis* (Daudin): A Systematical & Chronological Survey of the Development from the Fertilized Egg till the end of Metamorphosis (New York: Garland Publishing).
- Olson, S.Y., and Garban, H.J. (2008). Regulation of apoptosis-related genes by nitric oxide in cancer. *Nitric Oxide* *19*, 170–176.
- Ossipova, O., Dhawan, S., Sokol, S., and Green, J.B. (2005). Distinct **PAR-1** proteins function in different branches of Wnt signaling during vertebrate development. *Dev. Cell* *8*, 829–841.
- Peunova, N., Scheinker, V., Ravi, K., and Enikolopov, G. (2007). Nitric oxide coordinates cell proliferation and cell movements during early development of *Xenopus*. *Cell Cycle* *6*, 3132–3144.
- Poon, K.L., Richardson, M., Lam, C.S., Khoo, H.E., and Korzh, V. (2003). Expression pattern of neuronal nitric oxide synthase in embryonic zebrafish. *Gene Expr. Patterns* *3*, 463–466.
- Poon, K.L., Richardson, M., and Korzh, V. (2008). Expression of zebrafish *nos2b* surrounds oral cavity. *Dev. Dyn.* *237*, 1662–1667.
- Santagati, F., and Rijli, F.M. (2003). Cranial neural crest and the building of the vertebrate head. *Nat. Rev. Neurosci.* *4*, 806–818.
- Sharma, J.N. (2009). Hypertension and the bradykinin system. *Curr. Hypertens. Rep.* *11*, 178–181.
- Sive, H.L., Hattori, K., and Weintraub, H. (1989). Progressive determination during formation of the anteroposterior axis in *Xenopus laevis*. *Cell* *58*, 171–180.
- Sive, H.L., Grainger, R.M., and Harland, R.M. (2000). *Early Development of Xenopus laevis: A laboratory manual* (Cold Spring Harbor: Cold Spring Harbor Press).
- Spokony, R.F., Aoki, Y., Saint-Germain, N., Magner-Fink, E., and Saint-Jeannet, J.P. (2002). The transcription factor Sox9 is required for cranial neural crest development in *Xenopus*. *Development* *129*, 421–432.
- Theveneau, E., Steventon, B., Scarpa, E., Garcia, S., Trepas, X., Streit, A., and Mayor, R. (2013). Chase-and-run between adjacent cell populations promotes directional collective migration. *Nat. Cell Biol.* *15*, 763–772.
- Westerfield, M., Sprague, J., Doerry, E., and Douglas, S. (2001). The Zebrafish Information Network (ZFIN): a resource for genetic, genomic and developmental research. *Nucleic Acids Res.* *29*, 87–90.
- Westermann, D., Schultheiss, H.P., and Tschöpe, C. (2008). New perspective on the tissue kallikrein-kinin system in myocardial infarction: role of angiogenesis and cardiac regeneration. *Int. Immunopharmacol.* *8*, 148–154.
- Wiellette, E.L., and Sive, H. (2003). *vhnf1* and *Fgf* signals synergize to specify rhombomere identity in the zebrafish hindbrain. *Development* *130*, 3821–3829.
- Yan, Q., Feng, Q., and Beier, F. (2010). Endothelial nitric oxide synthase deficiency in mice results in reduced chondrocyte proliferation and endochondral bone growth. *Arthritis Rheum.* *62*, 2013–2022.
- Yu, H.S., Lin, T.H., and Tang, C.H. (2013). Bradykinin enhances cell migration in human prostate cancer cells through B2 receptor/PKC $\delta$ /c-Src dependent signaling pathway. *Prostate* *73*, 89–100.